J Infrared Milli Terahz Waves (2015) 36:1210–1220
DOI 10.1007/s10762-015-0210-4

Frequency Locking and Monitoring Based on Bi-directional Terahertz Radiation of a 3rd-Order Distributed Feedback Quantum Cascade Laser

N. van Marrewijk[1] · B. Mirzaei[1] · D. Hayton[2] · J. R. Gao[1,2] · T. Y. Kao[3] · Q. Hu[3] · J. L. Reno[4]

Received: 6 July 2015 / Accepted: 17 September 2015 /
Published online: 7 October 2015

Abstract We have performed frequency locking of a dual, forward reverse emitting third-order distributed feedback quantum cascade laser (QCL) at 3.5 THz. By using both directions of THz emission in combination with two gas cells and two power detectors, we can for the first time perform frequency stabilization, while monitor the frequency locking quality independently. We also characterize how the use of a less sensitive pyroelectric detector can influence the quality of frequency locking, illustrating experimentally that the sensitivity of the detectors is crucial. Using both directions of terahertz (THz) radiation has a particular advantage for the application of a QCL as a local oscillator, where radiation from one side can be used for frequency/phase stabilization, leaving the other side to be fully utilized as a local oscillator to pump a mixer.

Keywords Terahertz · Quantum cascade lasers (QCLs) · Frequency locking · Third-order distributed feedback

✉ B. Mirzaei
b.mirzaei@tudelft.nl

[1] Kavli Institute of Nanoscience, Delft University of Technology, Lorentzweg 1, 2628 CJ Delft, The Netherlands

[2] SRON Netherlands Institute for Space Research, Sorbonnelaan 2, 3584 CA Utrecht, The Netherlands

[3] Department of Electrical Engineering and Computer Science, Massachusetts Institute of Technology (MIT), Cambridge, MA 02139, USA

[4] Center for Integrated Nanotechnologies, Sandia National Laboratories, Albuquerque, NM 87185-0601, USA

1 Introduction

Terahertz (THz) quantum cascade lasers (QCLs) have been demonstrated as local oscillators for high-resolution spectroscopy both in the lab [1] and, more recently, in a real astronomic instrument [2]. In general, since the QCL is not inherently frequency stable, a system of frequency or phase locking [3, 4] is required. So far, the radiation emitted from only one direction of the QCL has been used for both pumping a mixer and stabilizing the frequency of the source [5]. In this way, to achieve frequency locking, part of the beam power is unavailable for the mixer. There have been many experiments to demonstrate the phase or frequency locking of a THz QCL [6–12]. For local oscillators operated at the high end of terahertz frequencies, such as for the astronomically important [OI] line at 4.7 THz, only two techniques are practically usable for frequency/phase locking since it can only be observed by an instrument in space. They are based on either a gas cell in combination with a THz power detector [10, 11] or a harmonic mixer [12]. The harmonic mixer down converts the QCL THz signal to one typically at MHz frequencies using the higher harmonic of a GHz local oscillator reference signal [12]. To realize the frequency locking, both techniques require a threshold power from a QCL, which can be comparable to what is needed for operating a superconducting mixer. In some cases, the power required for frequency locking can be half of the total power available from the laser making it very difficult to pump a mixer.

It is known that both a standard Fabry-Perot QCL and a distributed feedback (DFB) QCL can emit radiation from both forward and backward directions [13]. The beams in both directions are generated from a single oscillator, and therefore all the temporal characteristics are expected to be fundamentally the same. To take full advantage of the total radiating power available from a QCL, it is very beneficial to make use of the radiation from both directions. For example, one direction acts as a local oscillator source while the other is used for frequency or phase locking. This approach can also have other potential applications such as THz imaging radar [14]. Although it seems obvious that one should take advantage of both beams, in practice no one has ever reported the use of a QCL in this configuration as local oscillator at the high end of THz frequencies (e.g., 4.7 THz), where the available power is still relatively low.

In this paper, we develop a measurement setup that allows the detection of the radiation simultaneously from both directions. We start with the basic characterization of the radiation beam patterns and emitted power of a 3.5 THz, third-order DFB QCL [15]. We demonstrate a practical application of the dual emitting QCL by applying two gas cell-based frequency discriminators, one for each emission. Specifically, one side is used to realize frequency locking while the other side is used to monitor frequency stability. We find that the sensitivity of the detectors is crucial for both frequency locking and frequency monitoring. Finally, we describe briefly an experiment to make use of one side of radiation to carry out the frequency locking and the other side of the radiation to pump a superconducting niobium nitride (NbN) hot electron bolometer (HEB) mixer [16].

2 QCL and the Holder

We use a third-order DFB THz QCL based on a four-well resonant phonon depopulation design [17] developed at MIT (Fig. 1a). It emits a single mode at 3.490 THz, as measured by a Fourier transform spectrometer (FTS) with a resolution of 0.6 GHz. The device comprises 27

lateral corrugated grating periods over a ~1-mm-long active region, which is 10 μm thick and 50 μm wide. Multiple lasers are grouped together on a single chip, and the QCL used for our experiment is shown in Fig. 1a, where the QCL layout is perfectly symmetrical except that the bonding pad and wire appear only on one end of the laser. The third-order DFB structure [18–20], based on a linear phased antenna array concept, can have a controllable single emission mode as well as a low divergent far-field beam. Figure 1b schematically illustrates the laser on a chip that is mounted on a Cu chip holder. The latter is attached to a cold plate mounted on a cryocooler. Although the width of the cold plate, on top of which the laser holder is mounted, is larger than the length of the laser, due to a relative thick chip holder together with the fact that the beam can leave from the QCL chip at a positive angle ~5° [20], the reflection effects due to the presence of the cold plate are negligible. The radiation can therefore be emitted freely and simultaneously towards both directions.

3 Measurement Setup

The setup for the key measurement of this paper is illustrated in Fig. 2. The QCL is mounted in a pulse tube cryocooler that reaches ~4 K without load and typically ~12 K with the ~3-W electrical power dissipated by the QCL. The QCL is positioned in such a way where one end of the laser with the bonding pad and wire points to the backward direction. To allow both forward and backward radiation to exit the cryostat, two windows are installed. The front window (corresponding to the forward direction) is a 3-mm-thick high-density polyethylene (HDPE) with a transmission of 71 % measured at the laser frequency, while the rear window is a 1-mm-thick ultra-high molecular weight polyethylene (UHMW-PE) with a transmission of 89 % obtained at the same frequency. The QCL is placed in the center of the cryocooler with roughly an equal distance of ~ 80 mm to the windows.

Both forward and backward radiation are collimated by applying aluminum parabolic mirrors (f=80 mm) in front of each window and then reflected by flat mirrors through each of two gas cells with lengths of 41 and 27 cm, respectively. Note that the different lengths are not chosen on purpose but are due to their availability. Due to the abundance of absorption lines in the THz, methanol is used as the reference gas in both gas cells.

The forward radiation beam is then reflected by a flat mirror into a Si lens/antenna-coupled superconducting NbN HEB [1, 16], which is operated as a bolometric power detector. It

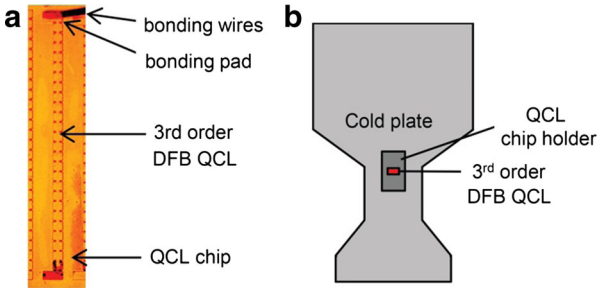

Fig. 1 **a** Photo of the third-order DFB QCL used for the experiment on a chip. One end of the laser with the bonding wire/pad is positioned towards the backward direction in the setup shown in Fig. 2. **b** Sketch of the QCL sample holder. The QCL (*red*) is mounted on a Cu chip holder (*dark gray*). The chip holder is attached to a cold plate (*light gray*) connected to a cryocooler

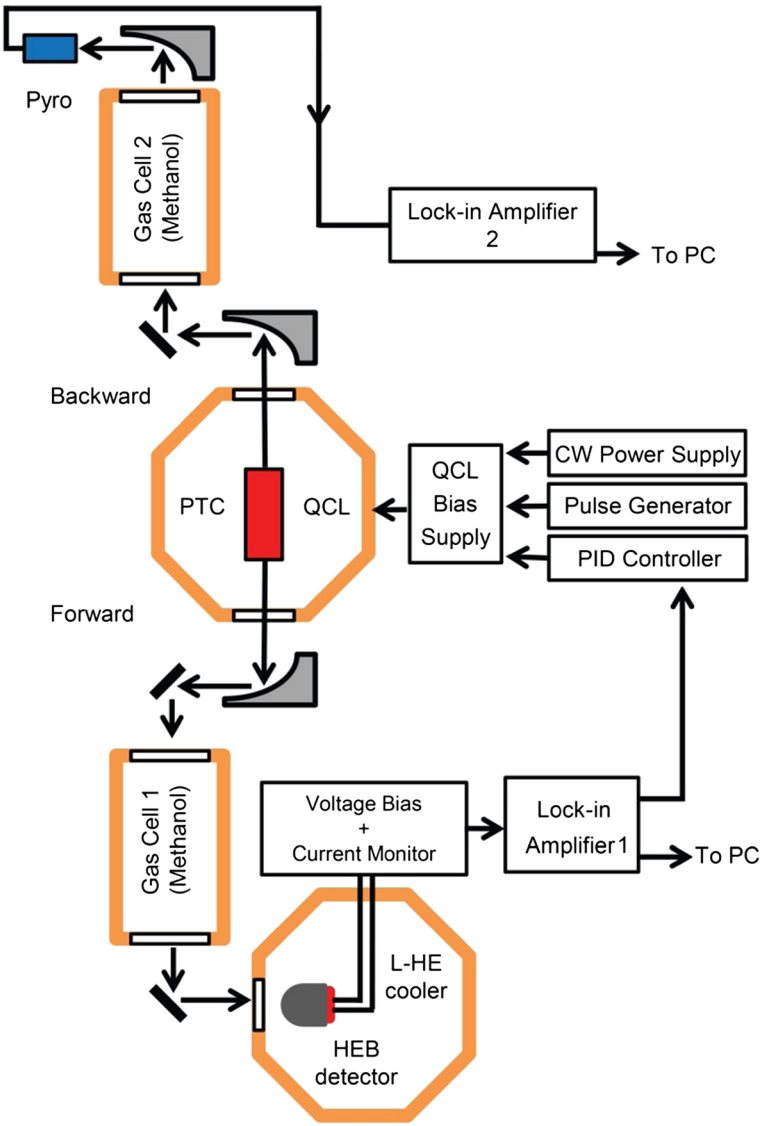

Fig. 2 Schematic of the measurement setup. The QCL is operated in a pulse tube cryocooler (PTC). The combination of a gas cell and a HEB detector is applied to generate an error signal to a PID controller for frequency locking (forward) and a second gas cell with a pyroelectric detector to monitor the quality of frequency locking (backward)

produces an error signal that is fed, via a lock-in amplifier, to a proportional integral derivative (PID) controller. The PID controller makes a correction signal that is added into the QCL bias voltage to hold the error signal at zero and therefore to stabilize the frequency. The feedback bandwidth, limited by the lock-in amplifier time constant, is ~10 Hz, although the PID bandwidth is much higher (~1 kHz). As indicated by the measured frequency noise power spectral density [11], a bandwidth of ~10 Hz is in practice sufficient to stabilize the average laser frequency and to remove low-frequency jitters.

The backward radiation beam after passing through the gas cell 2 is focused by an aluminum parabolic mirror (f=25 mm) onto a room temperature pyroelectric detector that is used for monitoring the quality of the frequency locking. We read out the signals from both detectors via two separate lock-in amplifiers connected to a PC. Since we have the same gas and roughly the same pressures in the gas cells, we expect to see a similar changing behavior from the signals detected by both detectors. The two detectors however have very different sensitivities. The HEB has a noise equivalent power (NEP) of 10^{-12}~10^{-13} [21], whereas the pyroelectric detector has a NEP of $\geq 10^{-9}$ [22]. Also, the former works at 4 K, while the latter operates at room temperature.

4 Experimental Results and Discussion

We start with the measurements of the far-field QCL beam patterns in both directions by using a small aperture pyroelectric detector scanned within a plane normal to the direction along the laser structure indicated in Fig. 2b (z-axis). The distance between the QCL and the scanned planes is about 90 mm. The laser was operated at a bias voltage of 14 V in a pulsed mode. We use this setting for all the measurements in this work except when specified otherwise. Figure 3 shows the measured beam patterns of the radiation from both directions.

We apply two methods to compare the powers between the radiation from the two directions. One is to estimate the relative powers by integrating the intensity of the entire beam. The other is to measure the relative powers by focusing the radiation into a pyroelectric detector. We find that the two directions give unequal powers, being independent of the methods used. The backward direction emits less power and has only 56 % power from the forward direction, obtained after correcting the effect due to two different transmissions of the windows. The difference by nearly a factor of 2 in power may be attributed to the bonding pad/wire on the laser in the backward direction. However, it requires additional work to confirm. The power result is consistent with the beam pattern measurement, where the S/N ratio is worse in the backward direction. We have not measured the absolute power of this particular laser since we are more interested in the ratio. However, based on the power measurement of a similar laser [5], we expect the maximal output power of the forward direction to be about 0.8 mW, while the other direction is 0.45 mW.

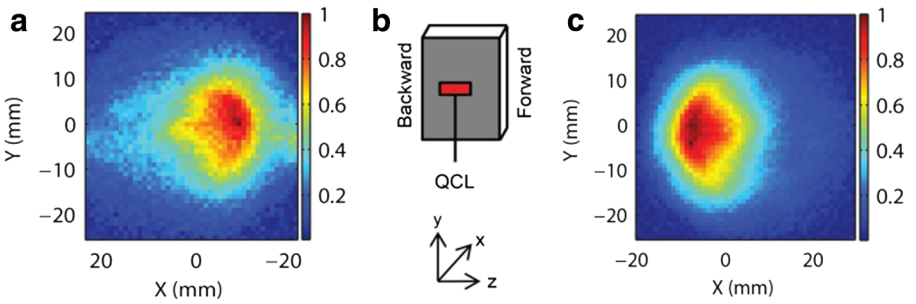

Fig. 3 **a** Measured beam pattern (normalized) from the backward radiation. The observation plane (x, y) is about 90 mm to the QCL. **b** Orientation of the QCL. The *arrows* indicate the positive x, y, and z directions. **c** Measured beam pattern (normalized) from the forward radiation. The observation plane (x, y) is also about 90 mm to the QCL

Prior to frequency locking, we measure methanol absorption lines by sweeping the QCL bias voltage from 13.5 to 14.5 V, which tunes the frequency electrically, as confirmed by a separate FTS measurement. Both gas cells are filled with methanol at a pressure of ~1.7 mbar. The transmitted signal intensity measured using both the HEB and the pyroelectric detector is plotted as a function of the QCL bias voltage in Fig. 4, where the signals are recorded with two lock-in amplifiers simultaneously.

The absorption lines, as expected when measuring with a single source, appeared at exactly the same bias voltages. The derivative of the absorption line at ~13.84 V was also measured by applying a small 70-Hz, 10-mVp-p AC modulation [10]. The resulting derivative curves for each detector is included as the inset in Fig. 4. The derivative curves change linearly with the QCL bias voltage over a range close to the absorption line center.

In this way, we can make use of an absorption line for frequency stabilization of the QCL because its frequency is known to be fundamentally stable [10, 11]. Any fluctuations in the frequency of the QCL below the bandwidth of ~10 Hz will cause proportional changes in the derivative output. In practice, we set the QCL bias voltage so as to have its frequency close to the center of a specific absorption line and then feed the derivative signal as the error input to the PID controller. The controller produces a feedback to the QCL bias voltage to keep its frequency aligned to the center of the absorption line where the derivative is equal to zero.

Now we focus on the key experiment of this paper using the setup in Fig. 2 by applying this method to gas cell 1 by feeding the HEB's derivative signal to the PID controller to stabilize the frequency, while utilizing output from the gas cell 2 to monitor the quality of frequency locking. A time series of the error signals measured simultaneously from both lock-in amplifiers is plotted in Fig. 5, where the upper panel shows the signal from the HEB and the lower panel shows the signal recorded by the pyroelectric detector.

In the time interval from 0 to 9 s (mode 1), the QCL was free running and the error signals recorded in both detectors are relatively large, which is primarily due to the ~1-Hz frequency of the pulse tube cooler. Low frequency drift noise is also visible. Afterwards (mode 2, 10–24 s), the PID is turned on reducing the error signal from the HEB by a factor of 20. It is generally accepted from the previous works [10, 11] that the QCL is then frequency locked. In the same time interval, the error signal from the pyroelectric detector is also reduced in comparison with the free running state. Although the fluctuations of the pyroelectric signal are around zero after the frequency locking, they are not as strongly suppressed as the

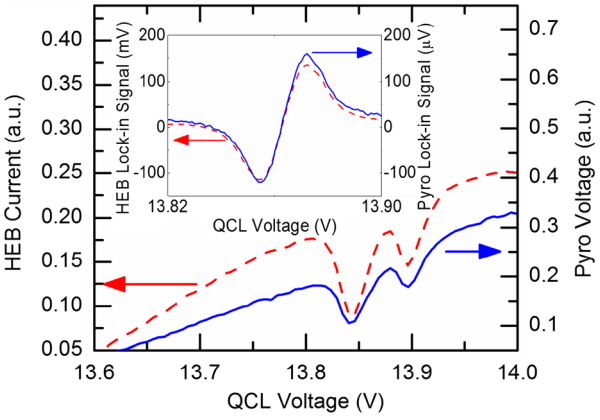

Fig. 4 Absorption lines of methanol at 1.7 mbar. The *lines* are measured with an HEB (*red dashed*) and a pyro (*blue*), respectively. The *inset* shows the derivative of an absorption line around 13.8 V measured with the HEB (*red dashed*) and the pyro (*blue*) by a lock-in amplifier when QCL is modulated with a small AC signal

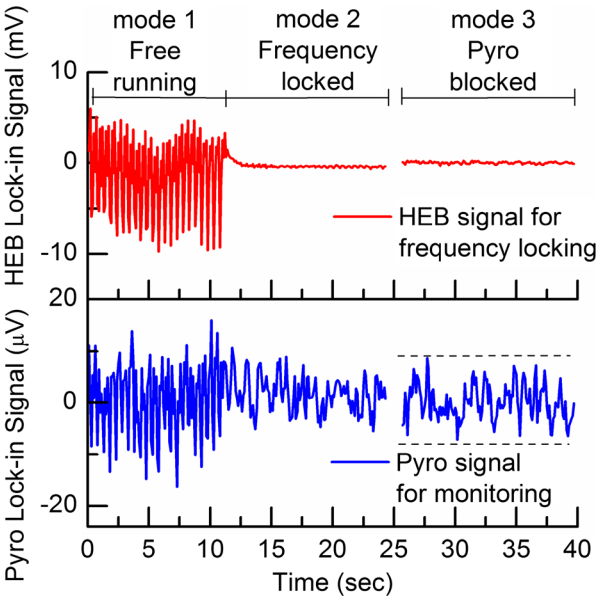

Fig. 5 The lock-in amplifier signal from the HEB (*top*, *red*) and the pyroelectric detector (*bottom*, *blue*), reflecting the frequency stability of the QCL. Frequency locking is engaged to the forward radiation after 12 s using the HEB signal (control), while the pyroelectric detector monitors the frequency of the backward radiation. After 30 s, the radiation to the pyroelectric detector is blocked. The *dashed line* represents the pyroelectric detector noise limit

fluctuations in the HEB. To understand this, we actually block the radiation to the pyroelectric detector and record its error signal, while the frequency locking is maintained by the HEB (referred as the mode 3 in Fig. 5). We find that the intrinsic noise level of the pyroelectric detector dominates in both cases, no matter whether there is a radiation signal to the pyroelectric detector or not. Thus, we realize that the error signal from the pyroelectric detector does not directly correspond to the frequency locking quality, but rather to the noise floor of the detector.

Due to the linearity of the derivative signal versus the QCL voltage curve, we can convert its fluctuation amplitude to frequency by making use of the voltage tuning coefficient of the laser [11]. The latter has roughly −0.6 GHz/V determined from a separate FTS experiment. We are therefore able to estimate a free running QCL linewidth of around 800 kHz, which is much larger than the intrinsic linewidth [23] because of time-dependent jitters. Strictly speaking, this is not the laser linewidth, but rather the range of laser emission frequency averaged in a measured time interval [11]. After turning the frequency locking on, this so-called linewidth is reduced to about 40 kHz. This analysis is based on the observation from the HEB. In contrast, if we make use of the error signal from the pyroelectric detector, we would record a linewidth of 300 kHz, which contradicts obviously with the first result.

To verify the importance of the noise level of the detector in such a frequency locking experiment, we modify the experiment slightly and take the error signal from the pyroelectric detector for the frequency locking and the HEB's signal for the monitoring. The results, plotted in the same manner as in Fig. 5, are shown in Fig. 6.

We now focus on the case of mode 2. The error signal from the pyroelectric detector has been reduced considerably relative to the free running case, and the signal is centered around zero. However, compared with the results by using the HEB for the frequency locking in Fig. 5, the residue on the locked signal is large. We attribute these fluctuations to the intrinsic noise of the pyroelectric detector. In this case, the PID controller cannot distinguish the changes between the QCL frequency and the noise from the detector. Consequently, the

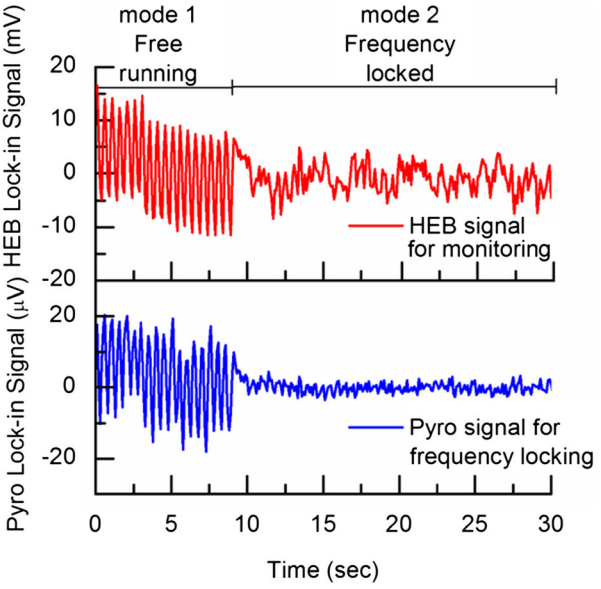

Fig. 6 The lock-in amplifier signal from the HEB (*top*, *red*) and the pyroelectric detector (*bottom*, *blue*) reflecting the frequency stability of the QCL. Frequency locking is engaged to the backward radiation after 9 s using the pyroelectric detector signal (control), while the HEB monitors the frequency of the forward radiation

feedback signal to the bias of the QCL cannot be appropriately applied. The lack of suppression in the frequency fluctuations can be monitored by the HEB. Since the (intrinsic) noise floor of the HEB is at least three or four orders of magnitude lower than that of the pyroelectric detector [21], the error signal in this case reflects more accurately the quality of the frequency locking. Because of the higher sensitivity of the HEB, these fluctuations are exclusively due to the frequency fluctuations of the QCL and they show only a mild reduction in the linewidth of the QCL. We perform the same analysis as before and find a free running linewidth of around 800 kHz. It becomes about 300 kHz in the locked situation when we use the HEB signal to assess the linewidth. From the pyroelectric detector signal, we would estimate roughly a 100-kHz linewidth. The small linewidth compared with the linewidth derived from the HEB may come from the fact that the PID controller adjusts the QCL frequency to remove the noise from the pyroelectric detector. This is why the HEB monitor shows more noise when the QCL is locked.

To explore the parameters of our experimental setup, we repeat the measurements a few times by adjusting three factors: the methanol pressure in the gas cells, the modulation frequency, and the modulation amplitude. We vary the pressure by a sub-mbar step and find that in the extreme case of very low pressures, the absorption lines become narrower, resulting in a very sharp derivative signal. This makes a more sensitive frequency discriminator but with reduced frequency bandwidth. In the opposite case of very high pressures, the absorption lines are too broad and the change in the error signal due to the change of the frequency is too weak. Then, the frequency locking becomes ineffective.

With respect to the modulation signal applied to the QCL bias voltage, we find that increasing the frequency can increase the *S*/*N* ratio, and reducing the amplitude helps to smooth the derivative signal. Both work well for the HEB case but not for the pyroelectric detector. As a compromise, we choose a relatively low modulation frequency of 70 Hz and relatively large amplitude of 10 mV to optimize the performance of the pyroelectric detector in the frequency locking experiments, while the HEB suffers slightly in its performance.

The consequence of the above choice is that in addition to the locked linewidth of 40 kHz and free running linewidth of 800 kHz, simultaneously the frequency of the laser is modulated by 6 MHz at a frequency of 70 Hz, which is calculated based on the voltage tuning coefficient of −0.6 GHz/V. Since a lock-in amplifier is used to demodulate the detector signal, the 70-Hz carrier is not visible in Figs. 5 and 6. This side effect is intrinsic to the gas cell technique [10, 11], although the effect can be made considerably weaker if one chooses a smaller modulation signal.

It is worthwhile to stress that our experiment represents the first one to make use of the bi-directional radiation from a single THz QCL for a frequency locking experiment, where the laser can be locked, while the quality of the locking can be evaluated in the same time. It is also the first to experimentally demonstrate the importance of the detector sensitivity in a frequency lock loop.

An interesting experiment that remains is to use the forward radiation for the frequency or phase locking for example and to use the backward radiation for monitoring if we can apply a second detector that is a low-noise HEB or a comparable detector. A different technique to monitor the linewidth on the other side after the locking could also be used. The latter can take advantage of a superlattice harmonic mixer, which can generate an ideal reference signal and mix it with the QCL signal into a microwave frequency [12], where one can directly record the linewidth by a spectrum analyzer.

A key demonstration of the advantage in using a dual emitting QCL is to show that a superconducting NbN HEB mixer can be appropriately pumped using one side of the laser while the other side is used for frequency locking. We perform such an experiment by using a standard NbN HEB mixer, which has a NbN area of 2 μm×0.2 μm, corresponding to a power requirement of 200 nW at the detector itself [1]. We apply a setup simplified with respect to the one in Fig. 2 by removing the gas cell 1 in the forward direction. We then lock the frequency of the QCL using the backward beam. At the same time, we apply the forward beam to pump the superconducting mixer. We find that it can pump the HEB to its nearly optimum operating points. With further optimization of the optics to match the beam to the HEB, we expect that the forward beam can provide sufficient power to pump the HEB to its optimum operating points, while the frequency locking is realized with the backward beam.

In this way, we can in essence make use of 100 % available power from a frequency-locked QCL. This approach is certainly beneficial for the case where a QCL is applied as a local oscillator for a superconducting mixer. This approach will be even more attractive for the cases where a QCL is applied as a local oscillator for a semiconductor Schottky mixer and an array of mixers, both of which require high power.

5 Conclusion

By making use of the radiation from the forward and backward directions of a third-order DFB QCL at 3.5 THz, we demonstrate for the first time that we can introduce the frequency locking, while can monitor the quality of the locking simultaneously. Furthermore, by applying two power detectors with a different noise level, we show that the frequency locking quality, namely the linewidth derived from the error signal, depends strongly on the noise level of the detector used. In the case of applying a high noise power detector for the locking, the PID controller not only corrects the frequency fluctuations of the laser but also compensates the

noise from the detector by adjusting the QCL frequency, which can lead to a much wider locked linewidth than what is indicated by the (locking) detector.

Acknowledgments The authors (B.M. and J.R.G.) acknowledge the support and encouragement from Leo Kouwenhoven. We also would like to thank Jerome Faist's group at ETH to help with making wire bonding to the laser for this experiment and Y. Ren for his advice on the use of the FTS. The work in the Netherlands is supported by NWO and NATO SFP. The work at MIT is supported by NASA and NSF. The work at Sandia was performed, in part, at the Center for Integrated Nanotechnologies, a US Department of Energy, Office of Basic Energy Sciences, user facility. Sandia National Laboratories is a multiprogram laboratory managed and operated by Sandia Corporation, a wholly owned subsidiary of Lockheed Martin Corporation, for the US Department of Energy National Nuclear Security Administration under contract DE-AC04-94AL85000.

References

1. J. L. Kloosterman, D. J. Hayton, Y. Ren, T. Y. Kao, J. N. Hovenier, J. R. Gao, T. M. Klapwijk, Q. Hu, C. K. Walker, and J. L. Reno, "Hot electron bolometer heterodyne receiver with a 4.7-THz quantum cascade laser as a local oscillator," *Appl. Phys. Lett.*, vol. 102, 011123, 2013.
2. H. Richter, M. Wienold, L. Schrottke, K. Biermann, H. T. Grahn and H. W. Hubers, "4.7-THz Local oscillator for the GREAT heterodyne spectrometer on SOFIA," *IEEE Trans. Terahertz Sci. Technol*., vol. 5, pp. 539-545, 2015.
3. A. L. Betz, R. T. Boreiko, B. S. Williams, S. Kumar, Q. Hu, and J. L. Reno, "Frequency and phase-lock control of a 3 THz quantum cascade laser," *Opt. Lett.*, vol. 30, no. 14, pp. 1837–1839, 2005.
4. M. Zhu and J. L. Hall, "Stabilization of optical phase/frequency of a laser system-application to a commercial dye laser with an external stabilizer," *J. Opt. Soc. Am. B*., vol. 10, pp. 802-816, 1993.
5. Y. Ren, D.J. Hayton, J.N. Hovenier, M. Cui, J.R. Gao, T.M. Klapwijk, S.C. Shi, T-Y. Kao, Q. Hu, and J.L. Reno, "Frequency and amplitude stabilized terahertz quantum cascade laser as local oscillator," *Appl. Phys. Lett.*, vol. 101, 101111, 2012.
6. A. Baryshev, J. N. Hovenier, A. J. L. Adam, I. Kašalynas, J. R. Gao, T. O. Klaassen, B. S. Williams, S. Kumar, Q. Hu, and J. L. Reno, "Phase locking and spectral linewidth of a two-mode terahertz quantum cascade laser," *Appl. Phys. Lett*., vol. 89, 031115, 2012.
7. D. Rabanus, U. U. Graf, M. Philipp, O. Ricken, J. Stutzki, B. Vowinkel, M. C. Wiedner, C. Walther, M. Fischer, and J. Faist, "Phase locking of a 1.5 Terahertz quantum cascade laser and use as a local oscillator in a heterodyne HEB receiver," *Opt. Express*, vol. 17, pp. 1159-1168, 2009.
8. P. Khosropanah, A. Baryshev, W. Zhang, W. Jellema, J. N. Hovenier, J. R. Gao, T. M. Klapwijk, D. G. Paveliev, B. S. Williams, S. Kumar, Q. Hu, J. L. Reno, B. Klein, and J. L. Hesler, "Phase locking of a 2.7 THz quantum cascade laser to a microwave reference," *Opt. Lett*., vol. 34, pp. 2958-2960, 2009.
9. L. Consolino, A. Taschin, P. Bartolini, S. Bartalini, P. Cancio, A. Tredicucci, H. E. Beere, D. A. Ritchie, R. Torre, M. S. Vitiello, P. De Natale, "Phase-locking to a free-space terahertz comb for metrological-grade terahertz lasers," *Nat. Commun*., vol 3, 1040, 2012.
10. H. Richter, S. G. Pavlov, A. D. Semenov, L. Mahler, A. Tredicucci, H. E. Beere, D. A. Ritchie, and H.-W. Hübers, "Submegahertz frequency stabilization of a terahertz quantum cascade laser to a molecular absorption line," *Appl. Phys. Lett*., vol. 96, 071112, 2010.
11. Y. Ren, J.N. Hovenier, M. Cui, D.J. Hayton, J.R. Gao, T.M. Klapwijk, S.C. Shi, T-Y. Kao, Q. Hu, and J. L. Reno, "Frequency locking of single-mode 3.5-THz quantum cascade lasers using a gas cell," *Appl. Phys. Lett*., vol. 100, 041111, 2012.
12. D. J. Hayton, A. Khudchencko, D. G. Pavelyev, J. N. Hovenier, A. Baryshev, J. R. Gao, T. Y. Kao, Q. Hu, J. L. Reno, and V. Vaks, "Phase locking of a 3.4 THz third-order distributed feedback quantum cascade laser using a room-temperature superlattice harmonic mixer," *Appl. Phys. Lett*., vol. 103, 051115, 2013.
13. B.S. Williams, "Terahertz Quantum-Cascade Lasers," *Nature Photon*., vol. 1, pp. 517-525, 2007.
14. K.B. Cooper, R.J. Dengler, N. Llombart, B. Thomas, G. Chattopadhyay, and P.H. Siegel, "THz Imaging Radar for Standoff Personnel Screening," *IEEE Trans. Terahertz Sci. Technol*., vol. 1, pp. 169-182, 2011.

15. M. I. Amanti, M. Fischer, G. Scalari, M. Beck, and J. Faist, "Low-divergence single-mode terahertz quantum cascade laser," *Nature Photon*., vol. 3, pp. 586-590, 2009.
16. J. R. Gao, M. Hajenius, Z. Q. Yang, J. J. A. Baselmans, P. Khosropanah, R. Barends, and T. M. Klapwijk, "Terahertz superconducting hot electron bolometer heterodyne receivers," *IEEE Trans. Appl. Supercond*., vol. 17, pp. 252-258, 2007.
17. Q. Qin, B. S. Williams, S. Kumar, J. L. Reno, and Q. Hu, "Tuning a Terahertz Wire Laser," *Nature Photon*., vol. 3, pp. 732-737. Nov. 2009.
18. M. I. Amanti, G. Scalari, F. Castellano, M. Beck, and J. Faist, "Low divergence Terahertz photonic-wire laser," *Opt. Express*, vol. 18, pp. 6390-6395, 2010.
19. Y. Kao, Q. Hu, and J. L. Reno, "Perfectly phase-matched third-order distributed feedback terahertz quantum-cascade lasers," *Opt. Lett*., vol. 37, pp. 2070-2072, 2012.
20. M. Cui, J. N. Hovenier, Y. Ren, N. Vercruyssen, J. R. Gao, T. Y. Kao, Q. Hu, and J. L. Reno, "Beam and phase distributions of a terahertz quantum cascade wire laser," *Appl. Phys. Lett*., vol. 102, 111113, 2013.
21. Y. Ren, W. Miao, Q. J. Yao, W. Zhang, and S. C. Shi, "Terahertz direct detection characteristics of a superconducting NbN bolometer," *Chin. Phys. Lett*., vol. 28, 010702, 2011.
22. R. N. Schouten, "A new amplifier design for fast low-noise far-infrared detectors using a pyroelectric element," *Meas Sci. Technol*., vol. 9, pp. 686-691, 1998.
23. M. S. Vitiello, L. Consolino, S. Bartalini, A. Taschin, A. Tredicucci, M. Inguscio, and P. De Natale, "Quantum-limited frequency fluctuations in a terahertz laser," *Nat. Photon.,* vol. 6, pp. 525-528, 2012.